

Supporting Information for:

Steam Stable Covalently-Bonded Polyethyleneimine
Modified Multiwall Carbon Nanotubes for Carbon
Dioxide Capture

*Zheng Zhou,[†] Santosh K. Balijepalli,[†] Anh H. T. Nguyen-Sorenson,[†] Clifton M. Anderson,[†]
Justin L. Park,[†] Kara J. Stowers^{*†}*

Corresponding Author

*Address correspondence to kstowers@chem.byu.edu

[†]Department of Chemistry and Biochemistry, Brigham Young University, Provo, UT 84602

Table of contents

Supplementary Figures and Tables

| | |
|-------------------|--|
| Figure S1. | SEM image with EDX of A) o-CNT and B) CNT-PEI |
| Table S1. | Functional group loading of CNT with various oxidative treatments |
| Figure S2. | A) Raman spectra and D/G ratios of CNT and o-CNT with various treatment times B) D/G ratios of CNT and o-CNT in relation to functional group loading |
| Figure S3. | The correlation of carboxylic acid group and functional group loading |
| Figure S4. | The relationship between calculated and experimental PEI loading |
| Table S2. | Statistical details of modal simulation from Rstudio |
| Table S2.A | The statistics model of the effect of functional group, surface area, pore volume and pore size on the covalent PEI loading of CNT |
| Table S2.B | Final possible regression models from Table S2.A |
| Table S3. | The effect of PEI concentration on PEI loading of o-CNT (Data for Figure 4) |
| Figure S5. | ^{13}C -NMR of PEI A) standard, B) treated with N_2 and C) treated with steam and N_2 at 120 °C for 24 h |

Discussion of Raman spectroscopy of CNT in relation to functional group loading

Discussion of CO_2 capture under dry and steam conditions

Tabulated values for Figures and breakthrough curves in the paper

| | |
|-------------------|---|
| Table S4. | Surface area and pore volume of CNT-PEI and CNT/PEI before and after (in parenthesis) steam treatment of the sorbents |
| Table S5. | The effect of treatment time on the functional group loading on CNT (Data for Figure 1) |
| Table S6. | The effect of functional group on PEI loading (Data for Figure 3A) |
| Table S7. | CO_2 capture of CNT, CNT-PEI and CNT/PEI without steam |
| Figure S6. | CO_2 capture breakthrough curve of CNT, covalently and physically PEI modified CNT |
| Figure S7. | TEM images and diameters of as is CNT and PEI-CNT |

References

Supplementary information

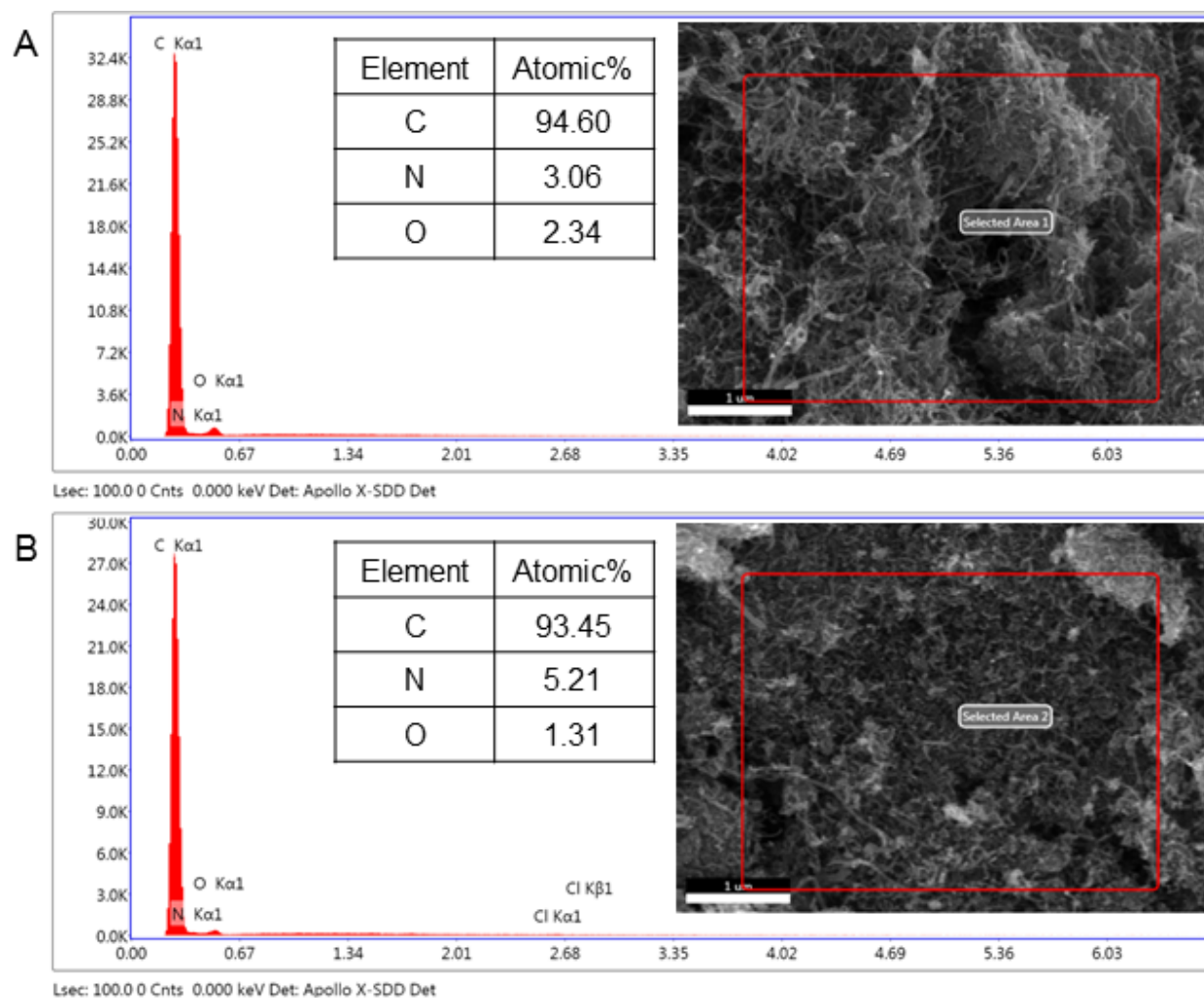


Figure S1. SEM image with EDX of A) o-CNT and B) CNT-PEI

Table S1. Functional group loading of CNT with various oxidative treatments

| Entry | Treatment | Time (h) | Functional group (wt%) |
|-------|---|----------|------------------------|
| 1 | As received | 0 | 1.27 |
| 2a | 16 M HNO ₃ 18 M H ₂ SO ₄ (3:1) | 3 | 2.44 |
| 2b | 16 M HNO ₃ 18 M H ₂ SO ₄ (3:1) | 16 | 2.46 |
| 3a | 16 M HNO ₃ | 3 | 1.85 |
| 3b | 16 M HNO ₃ | 16 | 4.66 |
| 3c | 16 M HNO ₃ | 24 | 6.5 |
| 3d | 16 M HNO ₃ (low temperature) | 24 | 5.28 |
| 4 | 3M HNO ₃ | 24 | 2.29 |

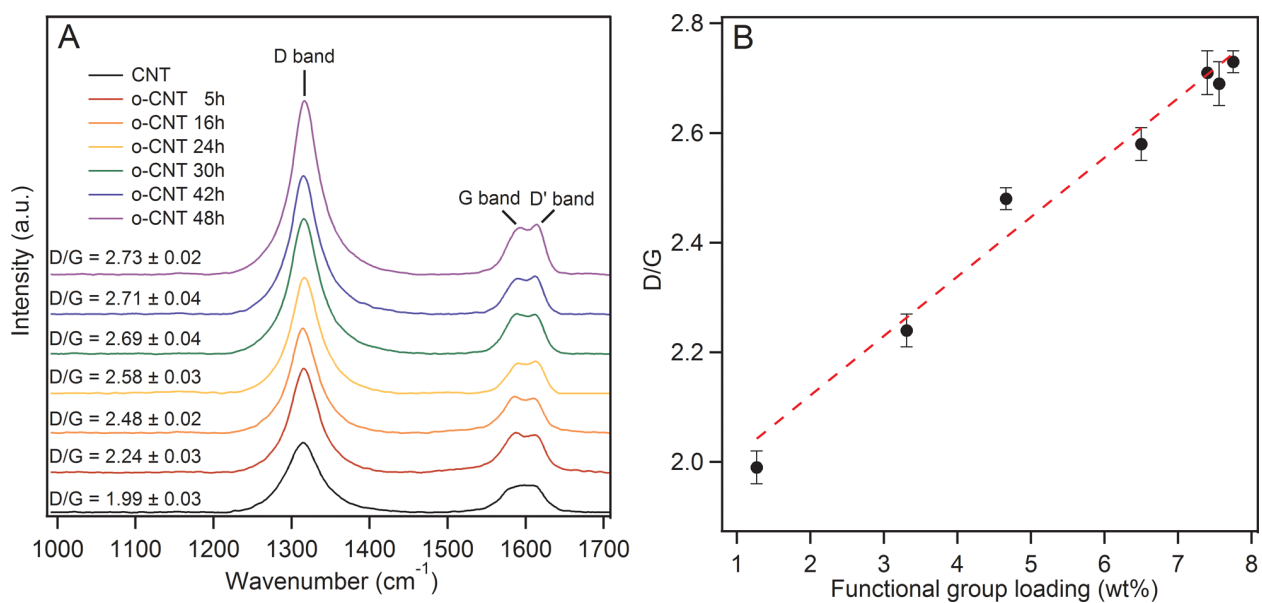


Figure S2. A) Raman spectra and D/G ratios of CNT and o-CNT with various treatment times B) D/G ratios of CNT and o-CNT in relation to functional group loading

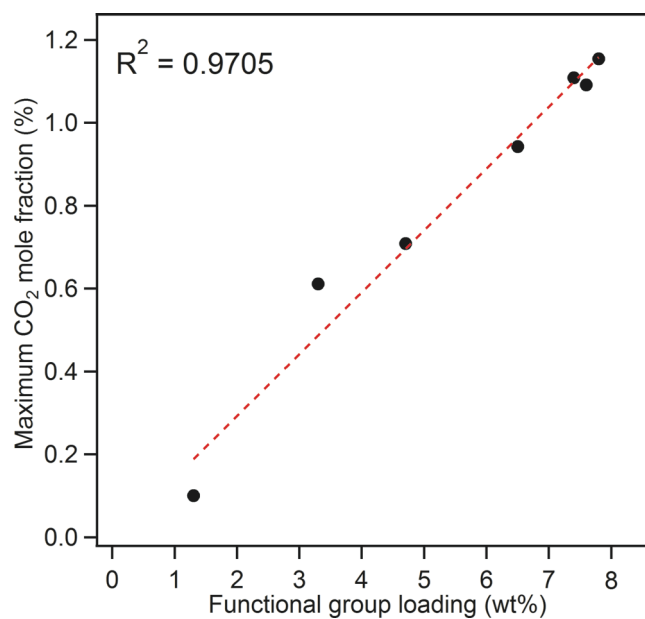


Figure S3. The correlation of carboxylic acid group and functional group loading

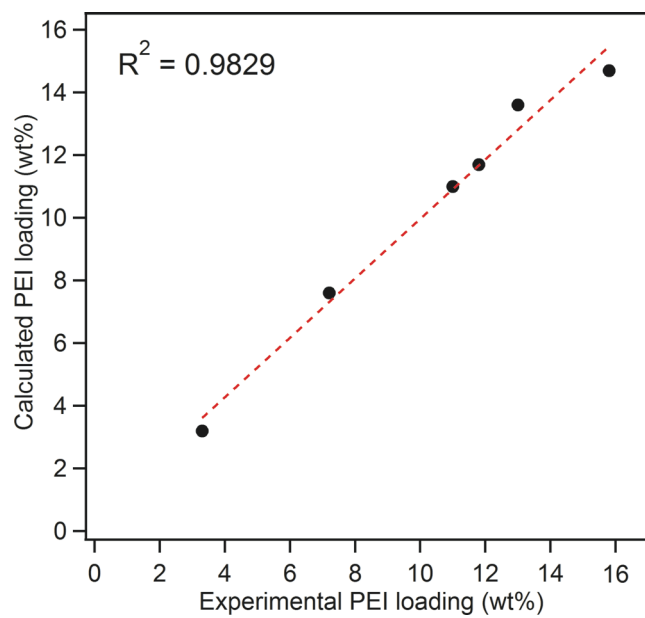


Figure S4. The relationship between calculated and experimental PEI loading

Table S2. Statistical details of modal simulation from Rstudio

| Summary ($\ln(\text{BPEI}) = \beta_0 + \beta_1 \cdot \text{Func} + \beta_2 \cdot \text{SA}$) | | | | |
|--|---|---------------------|----------|----------------|
| Coefficients: | Estimate | Std.Error | t value | Pr(> t) |
| (Intercept, β_0) | -0.073499 | 0.154134 | -0.48 | 6.66E-01 |
| Func, β_1 | 0.10292 | 0.014777 | 6.97 | 6.07E-03 ** |
| SA, β_2 | 0.012208 | 0.001346 | 9.07 | 2.83E-03 ** |
| Signif. codes: | 0 '***' 0.001 '**' 0.01 '*' 0.05 '.' 0.1 ' ' 1 | | | |
| Residual standard error: | 0.06233 on 3 degrees of freedom | | | |
| Multiple R-squared: | 0.9928 | Adjusted R-squared: | 0.988 | |
| F-statistic: | 206.6 on 2 and 3 DF | p-value: | 6.12E-04 | |

A multiple linear regression model was built to investigate the significant factors (PEI loading, surface area, pore volume and pore size) on the PEI loading. We built two full models and 20 reduced models to study the relationship between BPEI loading or logarithm of BPEI and all the factors mentioned above. In the model, we use IPEI, FG, SA, PV and PS to describe logPEI, functional group, surface area, pore volume and pore size. The factors are in Table S3 below.

Table S2.A The statistics model of the effect of functional group, surface area, pore volume and pore size on the covalent PEI loading of CNT

| Entry | Model | p-value | R ² | FG (p-value) | SA (p-value) | PV (p-value) | PS (p-value) |
|--------------|--------------------------|---------|----------------|-----------------|-----------------|-----------------|-----------------|
| Full model_1 | PEI ~ FG + SA + PV + PS | 0.0376 | 0.999 | 0.0448* | 0.0787 | 0.0936 | 0.0713 |
| Red model_10 | PEI ~ FG + SA + PV | 0.0745 | 0.950 | 0.1950 | 0.8120 | 0.3840 | NA |
| Red model_11 | PEI ~ FG + SA + PS | 0.0437 | 0.971 | 0.1026 | 0.0932 | NA | 0.2009 |
| Red model_12 | PEI ~ FG + PV + PS | 0.0614 | 0.959 | 0.1340 | NA | 0.1340 | 0.5450 |
| Red model_13 | PEI ~ SA + PV + PS | 0.1845 | 0.873 | NA | 0.5190 | 0.6060 | 0.6670 |
| Red model_14 | PEI ~ FG + SA | 0.0231 | 0.919 | 0.1107 | 0.0991 | NA | NA |
| Red model_15 | PEI ~ FG + PV | 0.0119 | 0.948 | 0.0060** | NA | 0.0501 | NA |
| Red model_16 | PEI ~ FG + PS | 0.0670 | 0.835 | 0.1240 | NA | NA | 0.3500 |
| Red model_17 | PEI ~ SA + PV | 0.0541 | 0.857 | NA | 0.0277* | 0.3012 | NA |
| Red model_18 | PEI ~ SA + PS | 0.0584 | 0.849 | NA | 0.1060 | NA | 0.3330 |
| Red model_19 | PEI ~ PV + PS | 0.0674 | 0.835 | NA | NA | 0.1242 | 0.0347* |
| Full model_2 | IPEI ~ FG + SA + PV + PS | 0.0206 | 1.000 | 0.0522 | 0.0771 | 0.1173 | 0.1062 |
| Red model_20 | IPEI ~ FG + SA + PV | 0.0102 | 0.993 | 0.1240 | 0.1700 | 0.7730 | NA |
| Red model_21 | IPEI ~ FG + SA + PS | 0.0084 | 0.994 | 0.0907 | 0.0142 | NA | 0.5301 |
| Red model_22 | IPEI ~ FG + PV + PS | 0.0193 | 0.987 | 0.1760 | NA | 0.0330* | 0.3580 |
| Red model_23 | IPEI ~ SA + PV + PS | 0.0418 | 0.972 | NA | 0.4510 | 0.6340 | 0.7950 |
| Red model_24 | IPEI ~ FG + SA | 0.0006 | 0.993 | 0.0061** | 0.0028** | NA | NA |
| Red model_25 | IPEI ~ FG + PV | 0.0033 | 0.978 | 0.0016** | NA | 0.0154* | NA |

| | | | | | | | |
|--------------|----------------|--------|-------|---------|---------|---------|----------|
| Red model_26 | IPEI ~ FG + PS | 0.0888 | 0.801 | 0.2930 | NA | NA | 0.7860 |
| Red model_27 | IPEI ~ SA + PV | 0.0050 | 0.971 | NA | 0.0025* | 0.0529 | NA |
| Red model_28 | IPEI ~ SA + PS | 0.0058 | 0.968 | NA | 0.0151* | NA | 0.0622 |
| Red model_29 | IPEI ~ PV + PS | 0.0081 | 0.960 | NA | NA | 0.0210* | 0.0040** |
| Red model_30 | IPEI ~ FG | 0.0170 | 0.795 | 0.0170* | NA | NA | NA |
| Red model_31 | PEI ~ FG | 0.0220 | 0.768 | 0.022* | NA | NA | NA |

*significant, **very significant

Since the mechanism (Scheme 1) showed PEI is covalently bonded to COOH groups on CNT, the functional group loading (FG) has to be included in the model. All models without FG factors are removed from the Table 1 (all red lines). Secondly, the FG factor should have significant effect on the PEI loading, which means the p-value of FG should be less than 0.05; all FG p-value higher than 0.05 are removed (all blue lines). All remaining factors in the model must be significant; therefore any model with an insignificant p-value factor is removed (green line). Finally, the experimental data should be well described by the model. Therefore, any model with relatively low R squared value (R^2) were removed (purple lines). The updated table is as follows:

Table S2.B Final possible regression models from Table S2.A

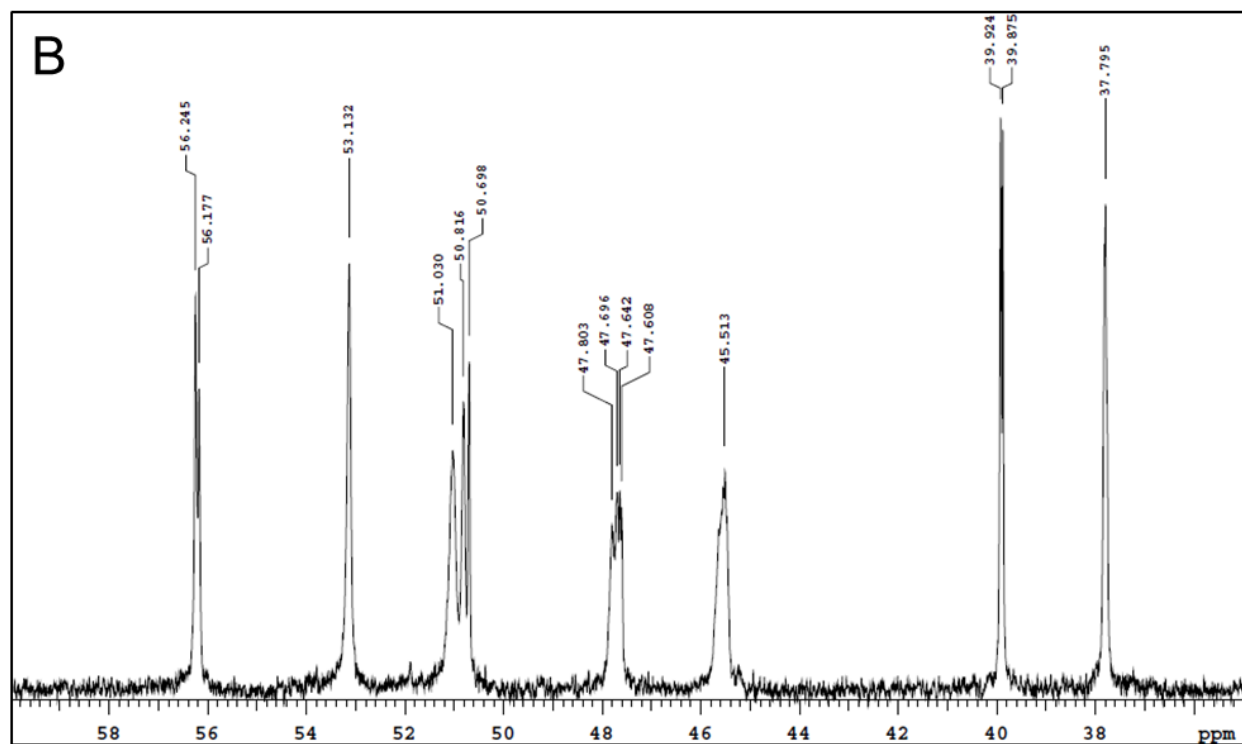
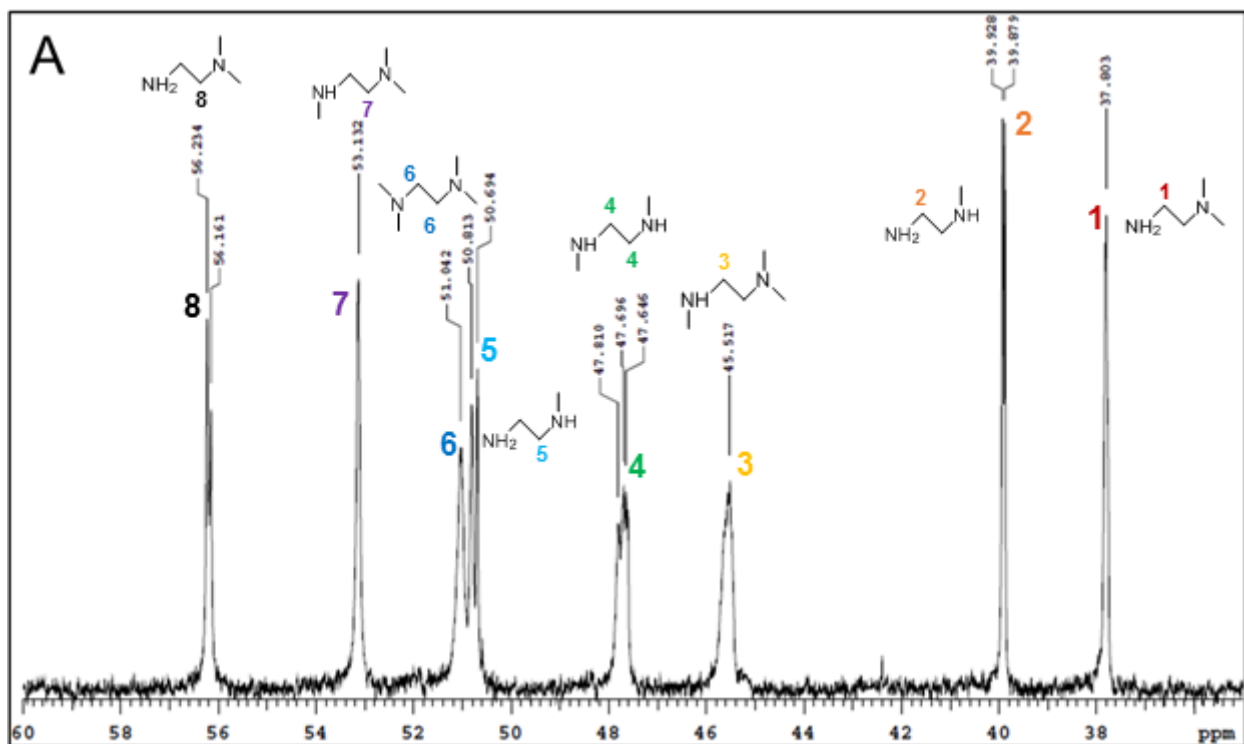
| Entry | Model | P-value | R^2 | FG | SA | PV | PS |
|--------------|----------------|---------|-------|----------|----------|---------|----|
| Red model_24 | IPEI ~ FG + SA | 0.0006 | 0.993 | 0.0061** | 0.0028** | NA | NA |
| Red model_25 | IPEI ~ FG + PV | 0.0033 | 0.978 | 0.0016** | NA | 0.0154* | NA |

*significant, **very significant

The resulting table showed only two models (Red model_24 and Red model_25) left. Besides FG, both SA and PV have a significant effect on the optimal covalent PEI loading. However, the effect of SA (**) was more significant compared to PV (*). Moreover, model_24 could better describe the experimental data compared to model_25 according to their R^2 values. In other research by Barron et. al, (ref.33) it was established that a large surface area is good for covalent attachment of organic molecules. Considering these three reasons, we proposed that SA and FG are the two major factors affecting the optimal covalent PEI loading on acid-treated CNT.

Table S3. The effect of PEI concentration on PEI loading of o-CNT

| PEI : o-CNT | | 0.25 | 1 | 2 | 3 |
|-------------|--------------------|-------|-------|-------|-------|
| PEI loading | No SOCl_2 | 3.1 | 3.29 | 2.81 | 2.51 |
| | SOCl_2 | 13.95 | 15.81 | 15.90 | 13.04 |



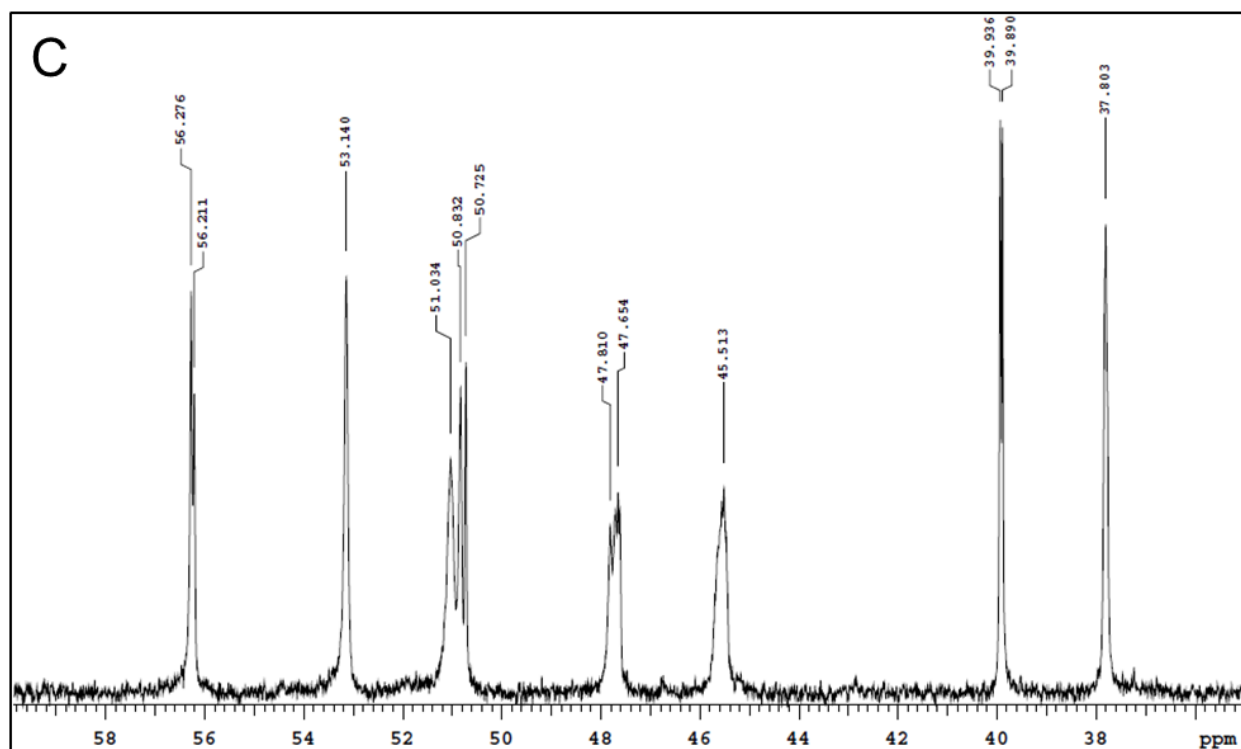


Figure S5. ^{13}C -NMR of PEI A) standard, B) treated with N_2 and C) treated with steam and N_2 at 120°C for 24 h

Table S4. Surface area and pore volume of CNT-PEI and CNT/PEI before and after (in parenthesis) steam treatment of the sorbents

| Material | Surface area (m^2/g) | Pore volume (cm^3/g) |
|----------|--|--|
| CNT/PEI | 26.28 (28.73) | 0.20 (0.36) |
| CNT-PEI | 54.10 (56.94) | 0.21 (0.21) |

Discussion of Raman spectroscopy of CNT in relation to functional group loading

Raman spectroscopy was used to investigate the degree of degradation of CNT in relation to the functional group loading measured by TGA. The intensity of the D band ($\sim 1320\text{ cm}^{-1}$) and the G band ($\sim 1585\text{ cm}^{-1}$) in Raman spectroscopy are related to the defects or disorder of graphitic structure and the sp^2 carbon graphitization of HNO_3 treated CNT (o-CNT) respectively (**Figure S2A**).^{1,2} D/G ratio was used to evaluate the degree of degradation where a higher value indicates a higher degree of functionalization on CNT while the D' band is a resonance feature.^{3,4} The results showed that the D/G ratio increased as treatment time increased, which indicates that in the range of 0 to 48 hours, extension of treatment times favors CNT structure degradation and functional group generation.^{5,6} The degradation of CNT decreased upon longer treatment times and did not show a significant change after 30 h. The total functional group loading measured by

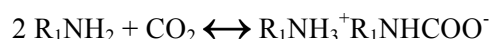
TGA was linearly related to D/G ratio ($R^2 = 98\%$), indicating the functional group generation is accompanied with CNT structure degradation (**Fig. S2B**).⁷

Discussion of CO₂ capture under dry and steam conditions.

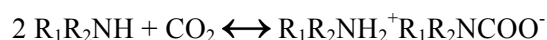
One CO₂ molecule is captured by two amine groups and form carbamates in dry conditions (1-2).⁸ In steam conditions, one CO₂ molecule is captured by only one amine group and form bicarbonate (3-5).^{9,10} Besides primary and secondary amines, tertiary amine can also capture CO₂ in steam conditions (5). Therefore, compared to dry conditions, CO₂ capture should be enhanced with steam.

CO₂ capture in dry conditions

(1) Primary amine:

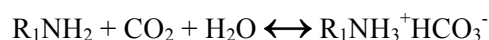


(2) Secondary amine:

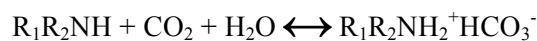


CO₂ capture in steam conditions

(3) Primary amine:



(4) Secondary amine:



(5) Tertiary amine:

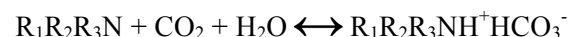


Table S5. The effect of treatment time on the functional group loading on CNT (Data for Fig. 1)

| Treatment time (h) | 0* | 5 | 16 | 24 | 30 | 42 | 48 |
|-------------------------|-----|-----|-----|-----|-----|-----|-----|
| Functional groups (wt%) | 1.3 | 3.3 | 4.7 | 6.5 | 7.6 | 7.4 | 7.8 |

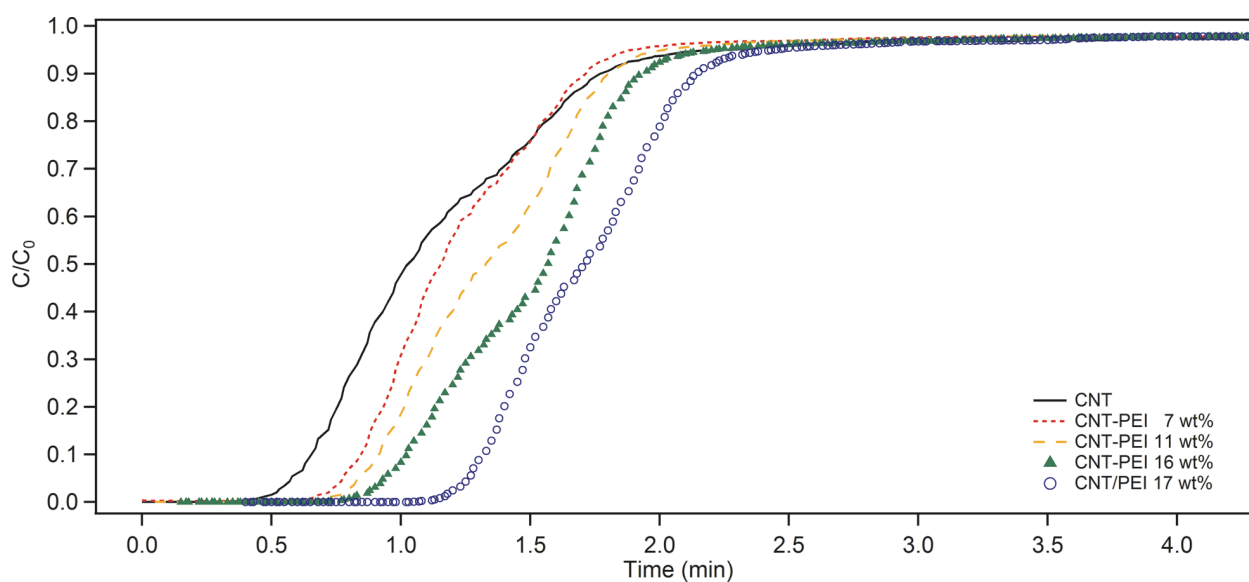
*CNT received as is

Table S6. The effect of functional group on PEI loading (Data for Fig. 3B)

| Functional group (wt%) | 1.3 | 2.3 | 3.3 | 4.7 | 5.3 | 6.5 | 7.7 | 7.8 |
|--------------------------------------|-----|-----|-----|------|------|------|------|------|
| PEI loading (wt%) | 3.3 | 5.0 | 7.2 | 11.0 | 14.0 | 15.8 | 13.0 | 11.8 |
| PEI loading standard deviation (wt%) | 0.1 | 0.2 | 0.2 | 0.2 | 0.4 | 0.1 | 0.4 | 0.4 |

Table S7. CO₂ capture of CNT, CNT-PEI and CNT/PEI without steam

| PEI loading (wt%) | CO ₂ capture (mmol/g) | Adsorbent |
|-------------------|----------------------------------|-----------|
| 0 | 0.284 ± 0.011 | NA |
| 7 | 0.505 ± 0.007 | CNT-PEI |
| 11 | 0.697 ± 0.015 | CNT-PEI |
| 16 | 0.981 ± 0.010 | CNT-PEI |
| 17 | 1.328 ± 0.023 | CNT/PEI |

**Figure S6.** CO₂ capture breakthrough curve of CNT, covalently and physically PEI modified CNT

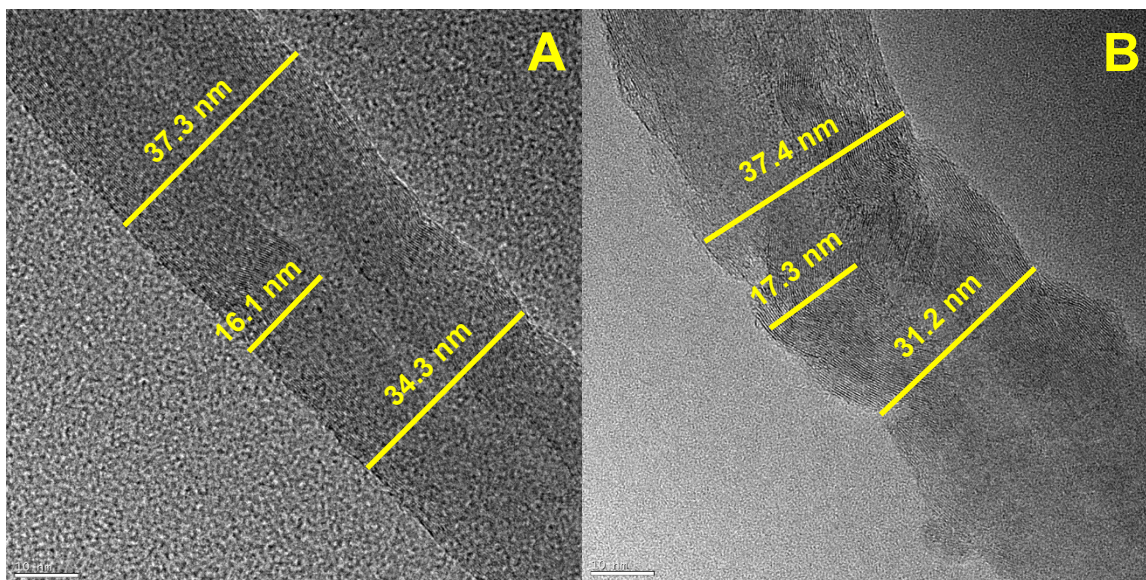


Figure S7. The TEM image and diameter of A) as is CNT and B) CNT-16wt%PEI

Reference

1. Van Thu, L.; Cao Long, N.; Quoc Trung, L.; Trinh Tung, N.; Duc Nghia, N.; Minh Thanh, V., Surface modification and functionalization of carbon nanotube with some organic compounds. *Adv. Nat. Sci-Nanosci.* **2013**, *4* (3), 035017 (5pp).
2. Kim, K. S.; Ryu, H.; Jang, G. E., Vertical growth of multi-walled carbon nanotubes by bias-assisted ICPHFCVD and their field emission properties. *Diam. Relat. Mater.* **2003**, *12* (10), 1717-1722.
3. Osorio, A. G.; Silveira, I. C. L.; Bueno, V. L.; Bergmann, C. P., H₂SO₄/HNO₃/HCl—Functionalization and its effect on dispersion of carbon nanotubes in aqueous media. *App. Surf. Sci.* **2008**, *255* (5, Part 1), 2485-2489.
4. Osswald, S.; Havel, M.; Gogotsi, Y., Monitoring oxidation of multiwalled carbon nanotubes by Raman spectroscopy. *J. Raman. Spectrosc.* **2007**, *38* (6), 728-736.
5. Elkashef, M.; Wang, K.; Abou-Zeid, M. N., Acid-treated carbon nanotubes and their effects on mortar strength. *Frontiers of Structural and Civil Engineering* **2016**, *10* (2), 180-188.
6. Tsai, P.-A.; Kuo, H.-Y.; Chiu, W.-M.; Wu, J.-H., Purification and Functionalization of Single-Walled Carbon Nanotubes through Different Treatment Procedures. *J. Nanomater.* **2013**, *2013*, 1-9.
7. Ma, P.-C.; Siddiqui, N. A.; Marom, G.; Kim, J.-K., Dispersion and functionalization of carbon nanotubes for polymer-based nanocomposites: A review. *A-Appl. S.* **2010**, *41* (10), 1345-1367.
8. Papavlu AP, Dinca V, Filipescu M, Dinescu M, Matrix-Assisted Pulsed Laser Evaporation of Organic Thin Films: Applications in Biology and Chemical Sensors. In *Laser Ablation - From Fundamentals to Applications*, p Ch. 08, Itina, T. E., Ed. InTech: Rijeka, 2017.
9. Mohammad, S. A.; Gasem, K. A. M., Multiphase Analysis for High-Pressure Adsorption of CO₂/Water Mixtures on Wet Coals. *Energy Fuels* **2012**, *26* (6), 3470-3480.
10. He, L.; Fan, M.; Dutcher, B.; Cui, S.; Shen, X.-d.; Kong, Y.; Russell, A. G.; McCurdy, P., Dynamic separation of ultradilute CO₂ with a nanoporous amine-based sorbent. *Chem. Eng. J.* **2012**, *189-190*, 13-23.